

1 **Stabilization of a Pickering emulsion by nanoparticles of Eudragit**
2 **RSPO and pol-epsilon caprolactone: Contact angle measurement**
3 **and surface tension studies**

4
5 *Abstract*

6 The use of colloidal particles to prepare and stabilize emulsions, known as "Pickering
7 emulsions", has aroused growing interest in recent years. Pickering and Ramsden
8 demonstrated at the beginning of the last century the feasibility of surfactant-free emulsions,
9 in presence of these emulsions is called "Pickering Emulsions". This concept of emulsions
10 stabilized by solid particles is experiencing renewed interest nowadays given the many
11 advantages it offers good stability, environmental protection, user safety, and particle
12 varieties.

13 The first part is devoted to the synthesis of Eudragit RSPO and pol epsilon-caprolactone
14 nanoparticles and their characterization. The characterization of the nanoparticles is
15 performed by dynamic light scattering and geometry. The understanding of the interfacial
16 behavior of these nanoparticles and their associated stabilization mechanisms for emulsions
17 was carried out. The second part of the study investigated the formulation and stabilization of
18 the emulsion using the washed suspension containing the nanoparticles as the only stabilizer.
19 The objective of this part is to stabilize and characterize the formulated emulsions. Droplet
20 size determination and microscopy were performed using a Zeiss optical microscope. The
21 direction of the formulated emulsions was determined by conductimetry. In conclusion,
22 Pickering emulsions stabilized solely by Eudragit RSPO and Poly-epsilon Caprolactone
23 nanoparticles appear to be highly effective innovative drug carriers, opening new doors as
24 potential drug delivery systems.

25 **Keywords:** Pickering Emulsion, Polymer, Contact angle, Eudragit RSPO, Poly-epsilon
26 Caprolactone

27

28 *Introduction*

29 The term emulsion has a very wide application and is usually difficult to identify with a
30 particular product. Emulsions are metastable mixtures of two immiscible liquids and an
31 amphiphilic agent. One of the liquids is dispersed in the other in the form of small spherical
32 drops whose size varies according to the conditions from 0.1 to a few tens of micrometers.
33 There are different types of emulsions: Water-in-oil emulsions where the dispersing phase,
34 also called the external phase or continuous phase, is constituted by the oil, and the internal
35 phase or discontinuous phase or dispersed phase is represented by the water; Oil-in-water
36 emulsions with the aqueous dispersing phase and the dispersed oily phase; Mixed emulsions
37 or multiple emulsions (W/O or O/W/O). The system thus created does not correspond to a
38 thermodynamically stable state, the most stable state would be the macroscopic separation of
39 the two fluids. Kinetic stability is ensured by the presence of amphiphilic molecules, called
40 emulsifiers, adsorbed at the interface between the two phases (Cabane and Henon, 2007).

41 These emulsifiers are most often surfactants. These are molecules with an affinity for both
42 water and oil. They are made up of a polar hydrophilic head and an apolar hydrophobic tail.
43 However, because they are harmful to the environment and the body, their use is not without
44 risk.

45 The use of colloidal particles to prepare and stabilize emulsions, known as 'Pickering
46 emulsions', has attracted increasing interest in recent years (Iwashita, 2020; Pickering, 1907).

47 These emulsions are called "Pickering emulsions". These emulsions are known in the
48 petroleum industry, food industry, and the design of inks, paints, and surfaces. Recently,

49 the possibilities of applications of particle-stabilized emulsions have been considered in the
50 pharmaceutical industry. This type of formulation can be a potential encapsulation system for
51 active ingredients, allowing the controlled and targeted release of the active from the internal
52 phase (Bago Rodriguez and Binks, 2019; Gonzalez Ortiz et al., 2020; Sy et al., 2020; Yang et
53 al., 2017; Zakir Hossain et al., 2021). However, this type of emulsion is not yet commercially
54 available. There are many studies on the formulation and physicochemical properties of
55 emulsions stabilized by solid particles, but to date studies in a biological environment have
56 not been described in the literature.

57 The control of the adsorption of colloidal particles at the liquid/ liquid interface leads to the
58 development of new functionalized. However, the study of the adsorption of colloidal
59 particles is very important to better understand their properties, materials such as
60 colloidosomes (Binks, 2017, 2007; Böker et al., 2007) as it can be, for instance, strong and
61 irreversible at the oil/water interface. The irreversible adsorption of the particles allows one to
62 obtain very stable emulsions (Binks, 2002; Binks and Horozov, 2005). This leads to the
63 formation of a dense film, thus creating a barrier around the droplets, giving them high
64 resistance to coalescence. The particle adsorption or desorption energy DE is mainly related
65 to their ability to be partially wetted by the two phases of the emulsion (Binks, 2007; Cayre et
66 al., 2012; Dickinson, 2010; Hunter et al., 2008). The particle wetting is characterized by the
67 contact angle between the aqueous phase, the oil phase, and the solid particles, measured on
68 the aqueous phase side, making the contact angle and the particle diameter two crucial
69 parameters to determine the interfacial adsorption forces. The well-documented literature in
70 this research area concerns, in most cases, the development of Pickering emulsions and
71 foams, and their potential use (Crossley et al., 2010; Dinsmore et al., 2002; Duan et al., 2005;
72 Velev et al., 1996; Wang et al., 2012; Yow and Routh, 2009).

73 The direct effect of the nanoparticles on the interfacial tension, which, is still in discussion, is
74 the “macroscopic”; the result of their impact on the formulation lies in their capabilities of
75 Pickering emulsion stabilization. The stabilization is generally higher when they form a dense
76 “monolayer” around the droplets, while partial coverage does not stabilize the emulsion
77 effectively because the “bald” plates favor the drainage of the film and
78 flocculation/coalescence. For this reason, it is acknowledged that better coverage is generally
79 obtained with smaller particles (Levine et al., 1989).

80 This work is devoted to the preparation and study of Pickering emulsions stabilized by a
81 polymer such as poly epsilon-caprolactone and eudragit RSPO. The work is divided into three
82 parts: first, the synthesis and characterization of nanoparticles for emulsion stabilization. Then
83 we carried out a formulation study including the determination of the contact angle and the
84 interfacial tension to better understand the stabilization mechanisms, and finally, the
85 preparation and characterization of the emulsions obtained.

86 **SECTION EXPERIMENTAL**

87 *Material and methods*

88 *1-1 Materials*

89 The equipment used for the synthesis and characterization of the nanoparticles is a Malvern
90 Zetasizer and a rotary evaporator. To measure the contact angle, we have developed an
91 experimental device. This device consists of an Optical bench, a light source, a thermostatic
92 tank filled with oil and a needle with a rising drop, a syringe filled with the aqueous phase, a
93 calibrated telecentric lens, a CCD camera, and a video monitor and a computer. A Wilhelmy
94 blade tensiometer (Dogno Abribat tensiometer) was used in the tensiometry study.

95

UNDER PEER REVIEW

97 **1-2 Regents**

98 The polymers used for the synthesis of the nanoparticles are poly epsilon-caprolactone (Sigma
99 Aldrich) and Eudragit RSPO (Rohm Germany), and the surfactant used is sodium dodecyl
100 sulfate (SDS) (LABOSI). As an aqueous phase, we used MilliQ water (Millipore). The
101 organic solvent used for the synthesis was acetone, Sigma Aldrich). Various other chemicals
102 were used.

103 **1-3 Methods**

104 **1-3-1 Synthesis and characterizations of nanoparticles**

105 Synthesis of poly epsilon-caprolactone and eudragit RSPO nanoparticles: The
106 nanoprecipitation technique, sometimes described as "solvent displacement", allows the
107 production of nanospheres or nanocapsules. It consists of dissolving the polymer in the
108 organic solution. The solvent chosen is generally a semi-polar solvent such as acetone or
109 ethanol, which must be miscible with water in all proportions. This solution is injected, with
110 moderate stirring, into an aqueous phase, possibly including sodium dodecyl sulphate, in
111 which the polymer is not soluble. The nanoparticles are then formed instantaneously under the
112 effect of the diffusion of the acetone toward the aqueous phase. The polymer, insoluble in the
113 water-solvent mixture, precipitates in the form of nanospheres. The organic solvent is then
114 removed by evaporation under reduced pressure.

115 Dynamic light scattering. Size distributions and poly- dispersity indices (PDI) were measured
116 by dynamic light scattering (DLS) with a NanoZS Malvern apparatus (Malvern, Orsay,
117 France). The helium/neon laser, 4 mW, was operated at 633 nm, with the scattering angle
118 fixed at 1731 and the temperature maintained at 25 1C. DLS data were analyzed using a
119 cumulant-based method, and experiments were performed in triplicate.

120 ζ Potential Measurements ζ were measured, with a NanoZS Malvern apparatus (Malvern,
121 Orsay, France). ζ potentials measurements were performed 1 h after formulation. The NanoZS
122 used in this study determined the electrophoretic mobility of the particle and then calculated
123 the values of ζ potential using teary's equation under the Smoluchowski approximation. All
124 experiments were performed in triplicate.

125 ***1-3-2 Contact angle measurement***

126 The contact angle measurement reports the ability of a liquid to spread on a surface by
127 wettability. The method consists of measuring the angle of the tangent of the profile of a drop
128 deposited on the substrate, with the surface of the substrate. It allows the surface energy of the
129 liquid or solid to be measured. The measurement of the contact angle gives access to the free
130 energy of a surface. It also allows the discrimination of the polar or apolar nature of the
131 interactions at the liquid-solid, liquid-liquid, and liquid-gas interface. The hydrophilic or
132 hydrophobic nature of a surface can thus be deduced.

133 To measure the contact angle we have developed an experimental device. This device consists
134 of an optical bench, light sources, thermostatic tanks filled with oil and needle with raising
135 drop, a syringe filled with the aqueous phase, calibrated telecentric lenses, CCD cameras, a
136 video monitor, and a computer. For drop formation, we have a system consisting of a
137 micrometric syringe with a volume of 1 ml, a silicone tube, and a stainless steel flat-tip needle
138 with an external diameter of 0.8 mm and an internal diameter of 0.5 mm. The drop images are
139 acquired by a CCD camera. They are then transmitted to a computer equipped with a graphics
140 card and Studio acquisition software. The images are then processed with Image J image
141 processing software. To obtain good image contrast, diffuse lighting is used. The intensity of
142 the lamp is set to its minimum. The optimal objective-drop distance x is about 13 cm; the best
143 compromise between magnification and image quality is then obtained. The camera-drop
144 distance x' is 30 cm, and the optical fiber-diffuser distance x' is 22 cm. The diffuser-drop

145 distance affects the contrast of the image obtained. The height of the millimetric syringe does
146 not influence the results but must be fixed during handling to avoid any instability.

147 The equipment used must be as clean as possible. The acquisition of the image of a drop is
148 done using the Studio software and the processing of this image to obtain the contact angle
149 using the ImageJ software. Before starting the measurements, it must be ensured that the
150 lamp, the camera, and the control screen are switched on. To obtain a sharp image of the drop,
151 it is advisable to place the camera lens approximately 13 cm from the drop.

152 Determination of the contact angle: Using Image J software

153 We use the Image J software to open the images and to measure a length or an angle. Opening
154 an image: File/Open and choose your image in the appropriate directory.

155 Measurement of a length: To measure the length of an image, you need a standard. So, on the
156 same image as what you want to measure, you must have a millimeter ruler or an object
157 whose size you know. In the rising drop experiment, a good standard is a syringe. To measure
158 the diameter of the drop, use the same method and note the length in pixels. Then, draw a
159 vertical line of the same length in pixels which will allow you to measure the diameter in the
160 right place. You can permanently draw this line by right-clicking/drawing or clearing.

161 Measuring an angle: To measure an angle, you must use the “Angle tool”. To measure the
162 angle between two lines, first, click on the two lines then at the intersection, hold the mouse
163 click and position it on the other line. The angle (“angle”) is then displayed in the main Image
164 J window.

165 *1-3-3 Tensiometer*

166 Interfacial tension is the free energy per unit area between two liquids (Cabane and Henon,
167 2007). It is called surface tension when one of the two liquids is gaseous. This interfacial

168 tension is measured using a tensiometer. Therefore, the main technique used in our study is
169 the Wilhelmy blade method.

170 In the case of the blade method, the liquid is brought into contact with a platinum blade (Pt),
171 itself connected to a precision balance. The force (F) necessary to tear the blade is measured
172 to determine the interfacial tension (according to the equation).

$$\gamma = \frac{F}{L \cos \theta}$$

173

174 γ : surface tension, F: surface tension force, L: length of the platinum plate, θ : contact angle A
175 Wilhelmy plate tensiometer (Dognon Abribat tensiometer) was used during this work. For
176 interfacial tension measurements, oil was gently added to the surface of the aqueous phase to
177 completely immerse the slide. The zero was performed before the measurement by immersing
178 the Wilhelmy blade in oil.

179 *1-3- 4 Formulation and characterizations of emulsion*

180 Macroscopic Examination: The emulsions are left to stand in the dark and at room
181 temperature in 15 ml conical tubes fitted with lids. This visual inspection highlights certain
182 phenomena of instability such as sedimentation, flocculation, and coalescence.

183 pH Determination: The determination of the pH of the solutions is based on the measurement
184 of the potential between two electrodes immersed in a solution rich in H⁺ ions After
185 calibrating the pH meter with solutions of known pH, the electrode is dipped into a 15 ml
186 conical tube containing the preparation to be studied. Like conductivity, care should be taken
187 to immerse the electrodes to the level of the emulsified phase for tubes with sedimentation.
188 The reading is made a few minutes after the insertion of the electrode.

189 Conductivity Measurement: It is based on the measurement of the electrical resistance of a
190 solution located between 2 plates covered with platinum black. Depending on the

191 concentration of ions present, the solution will have a greater or lesser conductivity. The
192 conductimetry cell is introduced into a 15 ml tube fitted with a screw-on lid containing the
193 preparation to be studied. In the presence of a conductive preparation, the conductivity meter
194 displays a value corresponding to the conductivity expressed in Siemens per meter (S. m⁻¹).
195 In the case of tubes with sedimentation, immerse the conductive cell to the level of the
196 emulsified fraction.

197 *Droplet Size of Pickering Emulsion:* a droplet of emulsion is placed on a slide and then
198 covered with a coverslip. The slide is placed on the stage of the microscope and the
199 observation is carried out with the 40X objective. The device is equipped with software that
200 allows direct photography of the observed image. The image of the droplets obtained
201 thereafter is correlated by the software which makes it possible to determine the size of the
202 droplets by delimiting the diameter of each droplet.

203

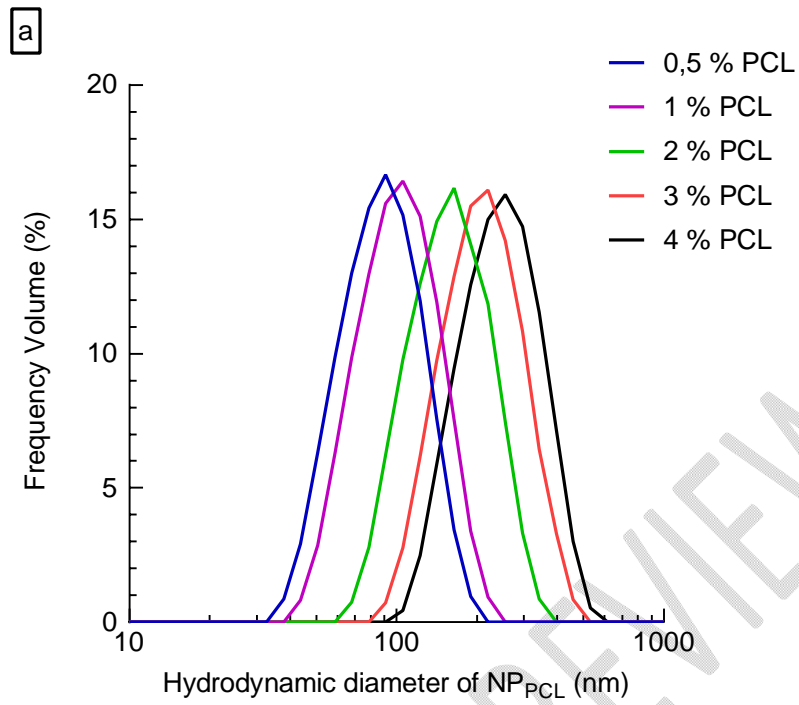
204 2- Results

205 2-1 Synthesis and characterization of nanoparticles

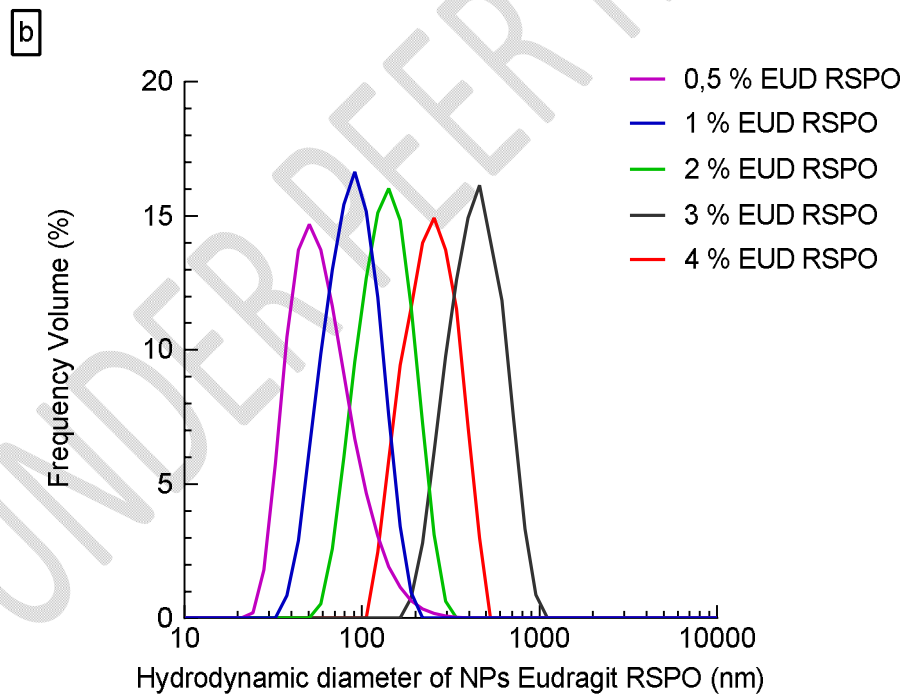
206 *Synthesis of poly epsilon-caprolactone and eudragit RSPO nanoparticles*

207 *Dynamic light scattering. Size distributions and poly- dispersity indices (PDI)*

208 We have developed nanoparticles by nanoprecipitation at different concentrations of polymers
209 0.5%, 1%, 2%, 3%, and 4% for eudragid RSPO and Poly epsilon-caprolactone. Figure 1
210 shows the size distribution of the nanoparticles. The size of the nanoparticles obtained varies
211 from 90 to 300 nanometers with polydispersity indices from 0.1 to 0.3.



212



213

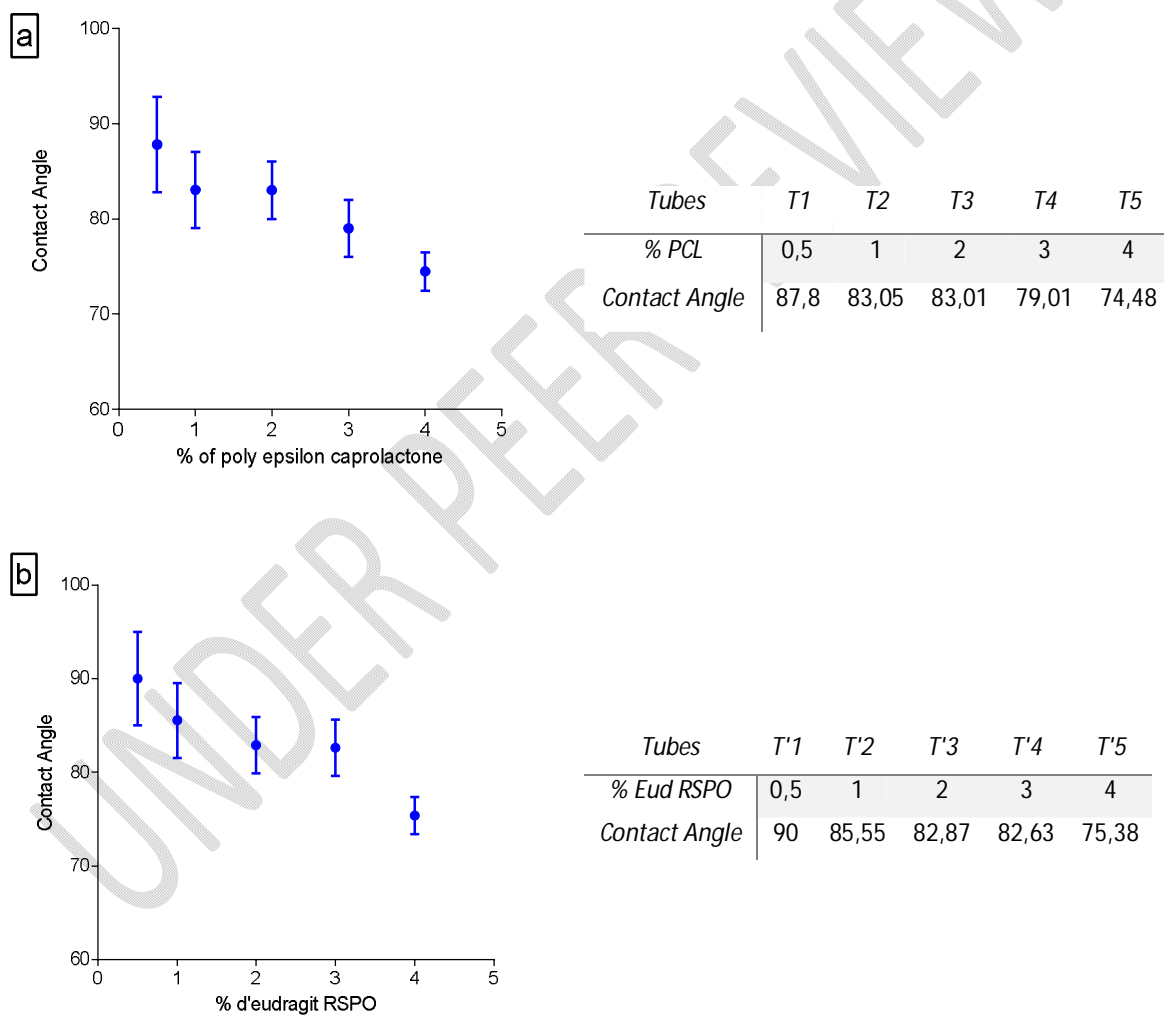
214 Figure1: hydrodynamic diameter of nanoparticles (a) pol epsilon-caprolactone (b) Eudragit

215 RSPO

216 Potential Measurements ζ : Le Potentiel Zeta déterminé pour le poly epsilon caprolactone
 217 nous donne des valeurs comprises entre -25 et -30 Mv et pour ceux de l'eudragit RSPO on a
 218 des valeurs comprises entre +20 et +40Mv.

219 2-2 Contact angle measurement

220 The following figures show the transformations of the image obtained with the assembly and
 221 the determination of the liquid-liquid contact angle by the Image J software. The results
 222 obtained are presented in Figures 2a and 2b.



223

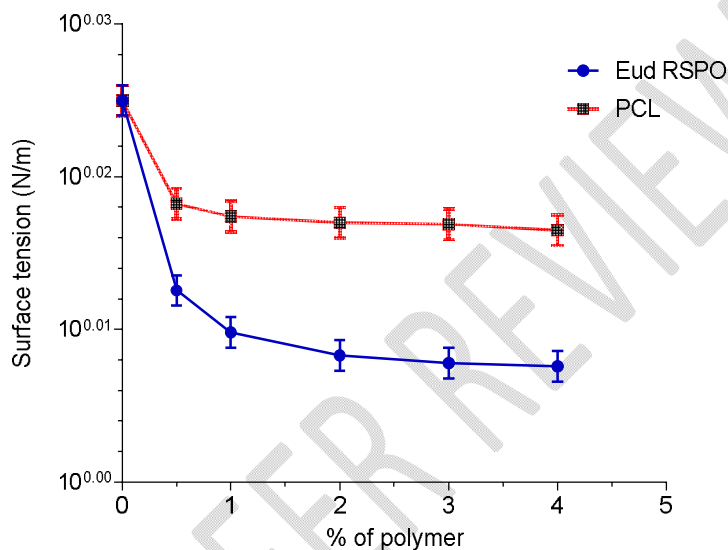
224 Figure 2: Contact angle (°) (a) Polyepsilon Caprolactone, (b) Eudragit RSPO.

225

226

2-3 Tensiometer studies

227 The surface tension measurements carried out show a lowering of the tension which is
228 conferred on the activity of the polymers at the water/oil interface. The reference voltage
229 without the nanoparticles being higher than that with the nanoparticles, Figure 3 shows the
230 results of the tensiometric studies:



231

232 Figure 3: Surface tension as a function of polymer percentage

233

2-4 Formulation and characterization of Pickering emulsion

234

Macroscopic Examination:

235

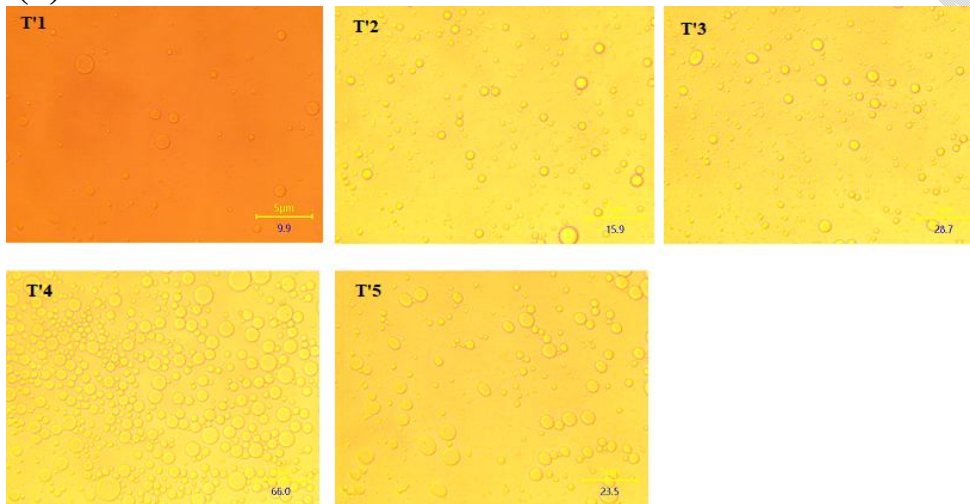
236 In this part, the study consisted in preparing a series of emulsions with the suspensions of
237 nanoparticles prepared (Eudragit RSPO and Poly Epsilon Caprolactone), to study their
238 stability. Except for the T1 tube, which has become destabilized since the first day after
239 preparation, and the T'1 tube, which has a dispersible cream by simple shaking, the emulsions
240 obtained have a white color and are stable. All the preparations (except tube 1 which is not
241 stable and tube 1' which presents a re-dispersible creaming by simple shaking), appear
242 macroscopically stable. That is to say that they do not show any destabilization phenomenon
visible to the naked eye at the end of the 28 days of storage.

243 Examen microscope

244 The microscopic examination with a ZEISS microscope shows us that these synthesized
245 particles are active at the water/oil interface and capable of stabilizing emulsions. The size
246 and density of the droplets depend on the quantity of polymer used for the synthesis of the
247 nanoparticles. Figures 4(a) and (b) show us the microscopic appearance of emulsion droplets.

248

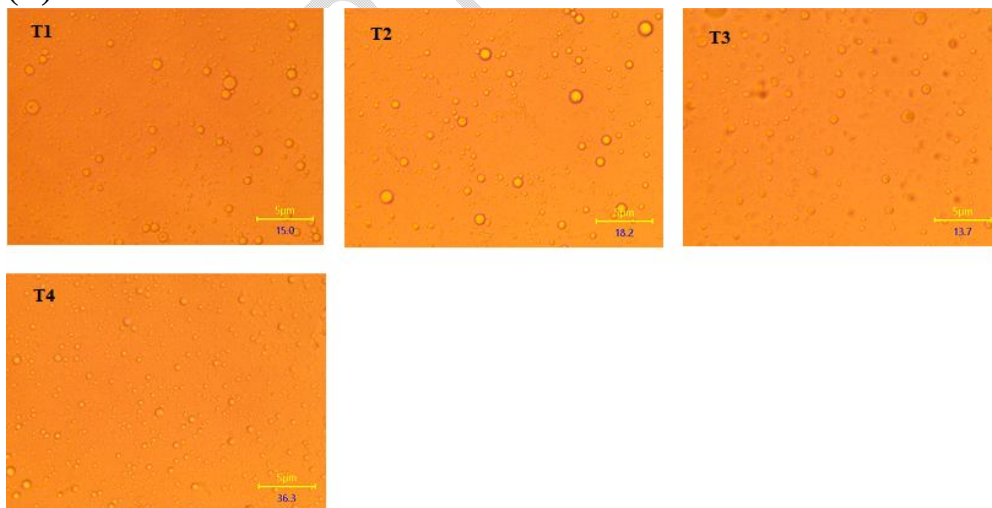
(a)



249

250

(b)



251

252 Figure 4: optical microscopy (a) emulsion stabilized by nanoparticles of Eudragit RSPO, (b)

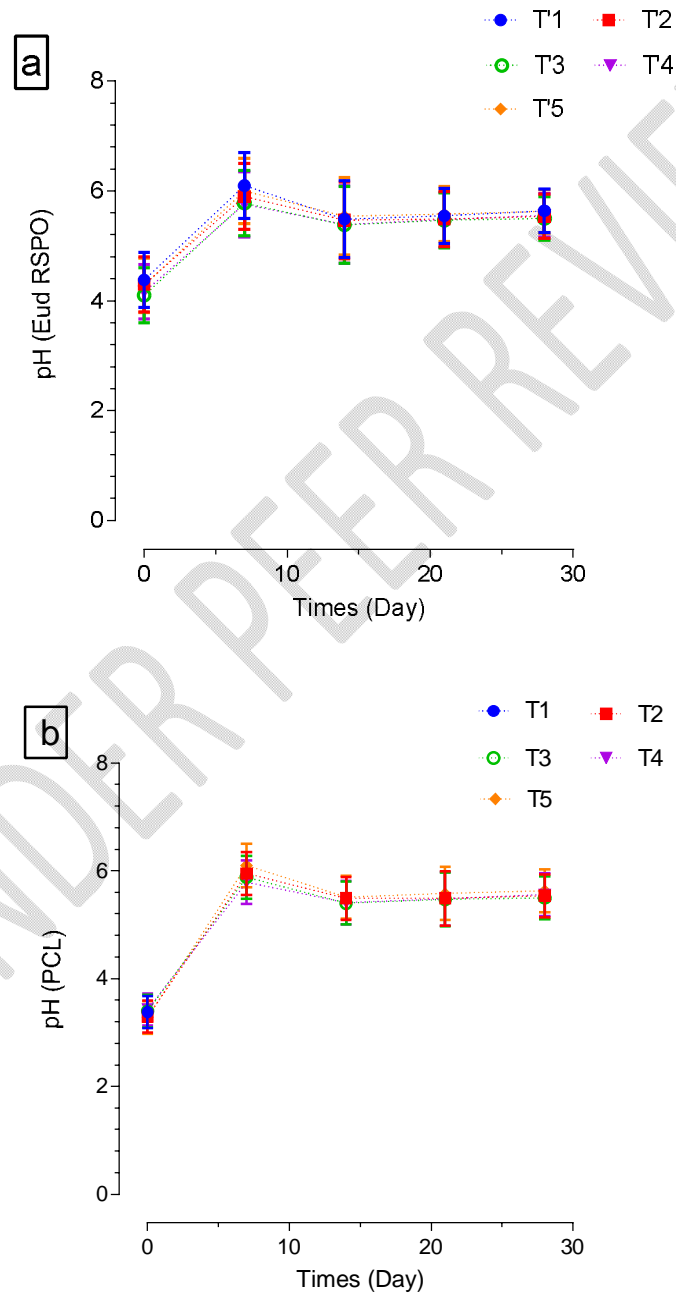
253

emulsion stabilized by nanoparticles of pol epsilon-caprolactone

254 *pH Determination:*

255 Les mesures de pH ont été réalisées à J1, J7, J14, J21. Les résultats sont représentés dans les
256 figures 5a et 5b ci-dessous.

257 The pH measurements were carried out on D1, D7, D14, and D21. The results are shown in
258 Figures 5a and 5b below.



259

Figure 5: pH of emulsions, (a) with Eudragit RSPO, (b) with pol epsilon-caprolactone

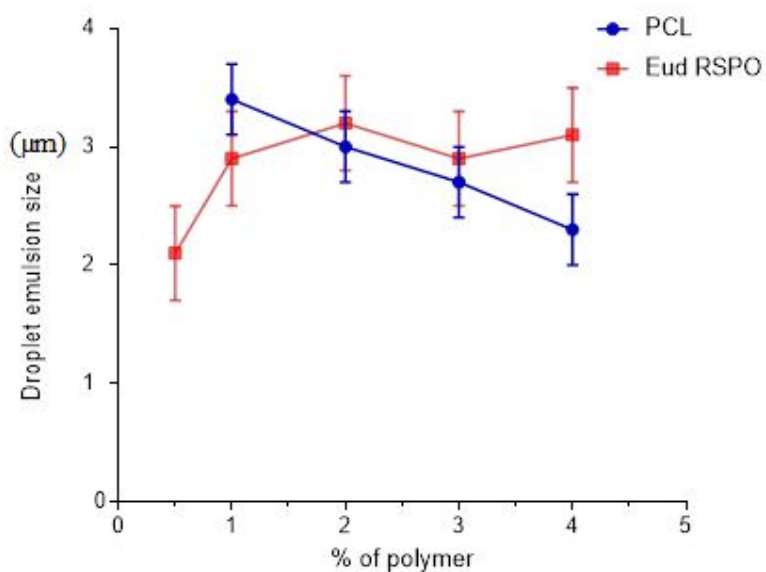
260

261 Conductivity Measurement:

262 The conductivity measurements were taken on D1, D7, D14, and D21. The results give
263 conductivity values of less than 0.02 mS/cm for all the preparations. The emulsions being
264 conductive, then we can confirm the direct direction of the emulsions obtained.

265 Droplet Size of Pickering Emulsion:

266 The measurement of the size of the droplets carried out on D15 after preparation shows the
267 results indicated in figure 6 As the T1 tube was not stable, we did not consider it necessary to
268 study the size of its droplets.



269

270 Figure 6: droplet size as a function of polymer percentage

271

272 **3- Discussion**

273 The main results obtained show that polymeric nanoparticles are potential candidates for
274 emulsion stabilization. Indeed, the replacement of solid particles with biodegradable organic
275 particles is an interesting prospect. This would make it possible to consider other routes of

276 application, for example, local injection (oral, subcutaneous, intramuscular). The absorption
277 of nanoparticles by intestinal cells is well known (Borm et al., 2006), so choosing a type of
278 particle without any possible toxicity is necessary.

279 In our context, which was emulsion stabilization by polymer nanoparticles, we demonstrated
280 the possibility of using poly epsilon-caprolactone and eudragit RSPO nanoparticles of size
281 between 90 and 300 nm and having stable emulsions. We prepared the emulsions by varying
282 the percentage of polymers to obtain suspensions of particles obtained by nanoprecipitation.

283 The study of the mechanisms of stabilization of emulsions by nanoparticles has become
284 essential. There are many studies on the mechanism of stabilization of Pickering emulsions by
285 ideally spherical particles and stabilization theories have been developed. In this study, we
286 studied the contact angle at the oil-water interface and the influence of nanoparticles on the
287 contact angle but also the surface tension between water and oil to see the influence of
288 nanoparticles. The drop in surface tension as a function of the percentage of nanoparticles
289 indicates an increase in the stability of the formulated emulsions.

290 The main results obtained about the physical properties showed that macroscopically, all the
291 formulations were stable during the first hours. Immediately afterward, the T1 tube
292 destabilized. For the T'1 tube, a re-dispersible cream was observed by simple agitation.

293 However, it should be kept in mind that these physical characteristics perceived with the
294 naked eye do not prejudge the stability of the emulsions obtained. Indeed, macroscopic
295 observation does not allow to see droplets smaller than 50 μm .

296 The determination of the direction of the emulsion was established thanks to the measurement
297 of the conductivity. The conductivity of the emulsions (all $<0.02\text{mS/cm}$) therefore confirms
298 their O/W nature. Indeed, the value of the conductivity of an emulsion depends on its external
299 phase (Redhead et al., 2001). The results thus obtained throughout the observation period
300 show that the emulsions did not undergo any phase inversion phenomenon.

301 Regarding the pH measurements, the results obtained indicated an acid character for all the
302 tubes. This acidity is unfavorable to the stability and preservation of the emulsions. The basic
303 nature gives the emulsions better stability. Yang and his collaborators showed that the
304 adjustment due to high values (9-12) allows a good stabilization of the emulsion by favouring
305 better adsorption of the particles at the interfaces (Rouzes et al., 2000). In addition, the pH
306 value of the emulsions influences its conservation and determines the incompatibilities that
307 there could be with the other components possibly present (Barbault-Foucher et al., 2002).

308 For all the preparations we used a fixed quantity of oil, the variable parameter being the
309 percentage of polymer used for the synthesis of the nanoparticles. We find that the size of the
310 droplets depends on the percentage of polymer used for the synthesis of the nanoparticles. As
311 for the size of the droplets, it plays an important role in the stability of emulsions and it is one
312 of the parameters that can modify the sedimentation rate described by Stokes' law (Binks and
313 Lumsdon, 2000; Hórvölgyi et al., 1996; Kabalnov and Wennerström, 1996; Langevin et al.,
314 2004), thus a 100-micrometer globule rises 10 cm in water in only 3 minutes, while it takes 5
315 hours and 20 days for globules respectively of 10 micrometers and 1 micrometer.

316 We observed that for all the tubes the average diameters are between 20 and 35 micrometers
317 For the tubes with the poly epsilon-caprolactone nanoparticles, a reduction in the average size
318 of the droplets is observed as a function of the percentage of polymer used for the synthesis of
319 the nanoparticles. Indeed, the most probable hypothesis would be, the increase in the number
320 of particles which would reduce the size of the droplets thus leading to an increase in the
321 interfacial zone (Langevin et al., 2004).

322 The relationship between the diameter and the number of particles is illustrated by the
323 following formula.

$$324 \quad D=(6\phi v V)/A$$

325 D is the diameter of the droplets

326 A/V is the interfacial area per unit volume

327 ϕ_v is the fraction of the dispersed phase

328 However, for emulsions stabilized by eudragit RSPO, this logic is not verified, we have
329 average sizes ranging from 2.1 to 3.2 μm (T1 (2.1 μm) T2 (2.9 μm) T3 (3.2 μm) T4(2.9 μm)
330 T5(3.1 μm)).

331 The results made it possible to obtain Pickering emulsions stabilized by nanoparticles of poly
332 epsilon-caprolactone and eudragit RSPO.

333

334

335

336 **4- Conclusion**

337 Unlike surfactant molecules which adsorb and desorb continuously, the particles adsorb at the
338 interfaces under the effect of agitation and irreversibly (the desorption energy of a particle is
339 of the order of $1500k_B T$ where k_B is the Boltzmann constant). We set ourselves the
340 objective of producing Pickering emulsions stabilized by polymeric nanoparticles of poly
341 epsilon-caprolactone and eudragit RSPO.

342 Of all the preparations, only T1 shows a phenomenon of instability and creaming for T1.
343 Conductive made-up emulsions are therefore of the O/W type. We had to note an acidity for
344 all the emulsions which is unfavorable for the stability of the latter. Compared to the two
345 batches, we observed that the size of the droplets is controlled by the number of nanoparticles.
346 Indeed, a high percentage of poly epsilon-caprolactone decreases the size of the emulsion
347 droplets. Also, the increase in the percentage of eudragit RSPO leads to a reduction in the size
348 of the droplets from 2%.

349 We also found that the amount of polymer used influences the value of the contact angle.

350 Indeed, the increase in the percentage of the polymer decreases the contact angle of the

351 emulsions. Better stability is noted with low surface tension values. The lower the surface
352 tension, the more stable the emulsion. This is why emulsions with eudragit RSPO are more
353 stable than those with poly epsilon-caprolactone. We can retain that the respect for various
354 physicochemical parameters makes it possible to guarantee better stability of the emulsions.
355 During this work all the emulsions prepared except for T1 are stable and those with eudragit
356 RSPO had better stability than emulsions with poly epsilon-caprolactone. The stability can be
357 improved by using a very high-speed stirrer for further work. The prospect of a double
358 encapsulation allowing a release in two stages, from nanoparticles and droplets, opens up the
359 prospects for significant therapeutic modulation. It would also be interesting to study the
360 incorporation of hydrophilic molecules in this type of formulation to determine their mode of
361 encapsulation in these particles and their release mechanisms.

362

363

364

365 *Références*

- 366 Bago Rodriguez, A.M., Binks, B.P., 2019. Capsules from Pickering emulsion templates.
367 *Current Opinion in Colloid & Interface Science*, Memorial Volume 44, 107–129.
368 <https://doi.org/10.1016/j.cocis.2019.09.006>
- 369 Barbault-Foucher, S., Gref, R., Russo, P., Guehot, J., Bochot, A., 2002. Design of poly-
370 epsilon-caprolactone nanospheres coated with bioadhesive hyaluronic acid for ocular
371 delivery. *J Control Release* 83, 365–375. [https://doi.org/10.1016/s0168-](https://doi.org/10.1016/s0168-3659(02)00207-9)
372 [3659\(02\)00207-9](https://doi.org/10.1016/s0168-3659(02)00207-9)
- 373 Binks, B.P., 2017. Colloidal Particles at a Range of Fluid–Fluid Interfaces. *Langmuir* 33,
374 6947–6963. <https://doi.org/10.1021/acs.langmuir.7b00860>

375 Binks, B.P., 2007. Colloidal particles at liquid interfaces. *Phys Chem Chem Phys* 9, 6298–
376 6299. <https://doi.org/10.1039/b716587k>

377 Binks, B.P., 2002. Particles as surfactants—similarities and differences. *Current Opinion in*
378 *Colloid & Interface Science* 7, 21–41. [https://doi.org/10.1016/S1359-0294\(02\)00008-0](https://doi.org/10.1016/S1359-0294(02)00008-0)

379 Binks, B.P., Horozov, T.S., 2005. Aqueous Foams Stabilized Solely by Silica Nanoparticles.
380 *Angewandte Chemie International Edition* 44, 3722–3725.
381 <https://doi.org/10.1002/anie.200462470>

382 Binks, B.P., Lumsdon, S.O., 2000. Effects of oil type and aqueous phase composition on oil–
383 water mixtures containing particles of intermediate hydrophobicity. *Phys. Chem.*
384 *Chem. Phys.* 2, 2959–2967. <https://doi.org/10.1039/B002582H>

385 Böker, A., He, J., Emrick, T., Russell, T.P., 2007. Self-assembly of nanoparticles at
386 interfaces. *Soft Matter* 3, 1231–1248. <https://doi.org/10.1039/B706609K>

387 Cabane, B., Henon, S., 2007. *Liquides : solutions, dispersions, émulsions, gels*. Belin.

388 Cayre, O.J., Hitchcock, J., Manga, M.S., Fincham, S., Simoes, A., Williams, R.A., Biggs, S.,
389 2012. pH-responsive colloidosomes and their use for controlling the release. *Soft*
390 *Matter* 8, 4717–4724. <https://doi.org/10.1039/C2SM00002D>

391 Crossley, S., Faria, J., Shen, M., Resasco, D.E., 2010. Solid nanoparticles that catalyze biofuel
392 upgrade reactions at the water/oil interface. *Science* 327, 68–72.
393 <https://doi.org/10.1126/science.1180769>

394 Dickinson, E., 2010. Food emulsions and foams: Stabilization by particles. *Current Opinion*
395 *in Colloid & Interface Science* 15, 40–49. <https://doi.org/10.1016/j.cocis.2009.11.001>

396 Dinsmore, A.D., Hsu, M.F., Nikolaidis, M.G., Marquez, M., Bausch, A.R., Weitz, D.A.,
397 2002. Colloidosomes: selectively permeable capsules composed of colloidal particles.
398 *Science* 298, 1006–1009. <https://doi.org/10.1126/science.1074868>

399 Duan, H., Wang, D., Sobal, N.S., Giersig, M., Kurth, D.G., Möhwald, H., 2005. Magnetic
400 colloidosomes derived from nanoparticle interfacial self-assembly. *Nano Lett* 5, 949–
401 952. <https://doi.org/10.1021/nl0505391>

402 Gonzalez Ortiz, D., Pochat-Bohatier, C., Cambedouzou, J., Bechelany, M., Miele, P., 2020.
403 Current Trends in Pickering Emulsions: Particle Morphology and Applications.
404 *Engineering* 6, 468–482. <https://doi.org/10.1016/j.eng.2019.08.017>

405 Hórvölgyi, Z., Németh, S., Fendler, J.H., 1996. Monoparticulate Layers of Silanized Glass
406 Spheres at the Water–Air Interface: Particle–Particle and Particle–Subphase
407 Interactions. *Langmuir* 12, 997–1004. <https://doi.org/10.1021/la940658o>

408 Hunter, T.N., Pugh, R.J., Franks, G.V., Jameson, G.J., 2008. The role of particles in
409 stabilizing foams and emulsions. *Adv Colloid Interface Sci* 137, 57–81.
410 <https://doi.org/10.1016/j.cis.2007.07.007>

411 Iwashita, Y., 2020. Pickering–Ramsden emulsions stabilized with chemically and
412 morphologically anisotropic particles. *Current Opinion in Colloid & Interface Science,*
413 *Emulsions and Microemulsions* 49, 94–106.
414 <https://doi.org/10.1016/j.cocis.2020.05.004>

415 Kabalnov, A., Wennerström, H., 1996. Macroemulsion Stability: The Oriented Wedge
416 Theory Revisited. *Langmuir* 12, 276–292. <https://doi.org/10.1021/la950359e>

417 Langevin, D., Poteau, S., Hénaut, I., Argillier, J.F., 2004. Crude Oil Emulsion Properties and
418 Their Application to Heavy Oil Transportation. *Oil & Gas Science and Technology -*
419 *Rev. IFP* 59, 511–521. <https://doi.org/10.2516/ogst:2004036>

420 Levine, S., Bowen, B.D., Partridge, S.J., 1989. Stabilization of emulsions by fine particles II.
421 capillary and van der Waals forces between particles. *Colloids and Surfaces* 38, 345–
422 364. [https://doi.org/10.1016/0166-6622\(89\)80272-0](https://doi.org/10.1016/0166-6622(89)80272-0)

423 Pickering, S.U., 1907. CXCVI.—Emulsions. *J. Chem. Soc., Trans.* 91, 2001–2021.
424 <https://doi.org/10.1039/CT9079102001>

425 Redhead, H.M., Davis, S.S., Illum, L., 2001. Drug delivery in poly(lactide-co-glycolide)
426 nanoparticles surface modified with poloxamer 407 and poloxamine 908: in vitro
427 characterization and in vivo evaluation. *Journal of Controlled Release* 70, 353–363.
428 [https://doi.org/10.1016/S0168-3659\(00\)00367-9](https://doi.org/10.1016/S0168-3659(00)00367-9)

429 Rouzes, C., Gref, R., Leonard, M., De Sousa Delgado, A., Dellacherie, E., 2000. Surface
430 modification of poly(lactic acid) nanospheres using hydrophobically modified
431 dextrans as stabilizers in an o/w emulsion/evaporation technique. *Journal of*
432 *Biomedical Materials Research* 50, 557–565. [https://doi.org/10.1002/\(SICI\)1097-](https://doi.org/10.1002/(SICI)1097-4636(20000615)50:4<557::AID-JBM11>3.0.CO;2-R)
433 [4636\(20000615\)50:4<557::AID-JBM11>3.0.CO;2-R](https://doi.org/10.1002/(SICI)1097-4636(20000615)50:4<557::AID-JBM11>3.0.CO;2-R)

434 Sy, P.M., Diouf, L.A.D., Djiboune, A.R., Dieng, S.M., Soumboundou, M., Diop, C., Diop, T.,
435 Mbaye, G., Mbodj, M., Diarra, M., 2020. pH-sensitive Pickering Emulsion Stabilized
436 by Hydroxyapatite Nanoparticles: Stability and Controlled Release Study. *European*
437 *Journal of Biophysics* 8, 52. <https://doi.org/10.11648/j.ejb.20200802.16>

438 Velev, O.D., Furusawa, K., Nagayama, K., 1996. Assembly of Latex Particles by Using
439 Emulsion Droplets as Templates. 1. Microstructured Hollow Spheres. *Langmuir* 12,
440 2374–2384. <https://doi.org/10.1021/la9506786>

441 Wang, Z., van Oers, M.C.M., Rutjes, F.P.J.T., van Hest, J.C.M., 2012. Polymersome
442 Colloidosomes for Enzyme Catalysis in a Biphasic System. *Angewandte Chemie*
443 *International Edition* 51, 10746–10750. <https://doi.org/10.1002/anie.201206555>

444 Yang, Y., Fang, Z., Chen, X., Zhang, W., Xie, Y., Chen, Y., Liu, Z., Yuan, W., 2017. An
445 Overview of Pickering Emulsions: Solid-Particle Materials, Classification,
446 Morphology, and Applications. *Front Pharmacol* 8, 287.
447 <https://doi.org/10.3389/fphar.2017.00287>

448 Yow, H.N., Routh, A.F., 2009. Release Profiles of Encapsulated Actives from Colloidosomes

449 Sintered for Various Durations. *Langmuir* 25, 159–166.

450 <https://doi.org/10.1021/la802711y>

451 Zakir Hossain, K.M., Deeming, L., J. Edler, K., 2021. Recent progress in Pickering emulsions

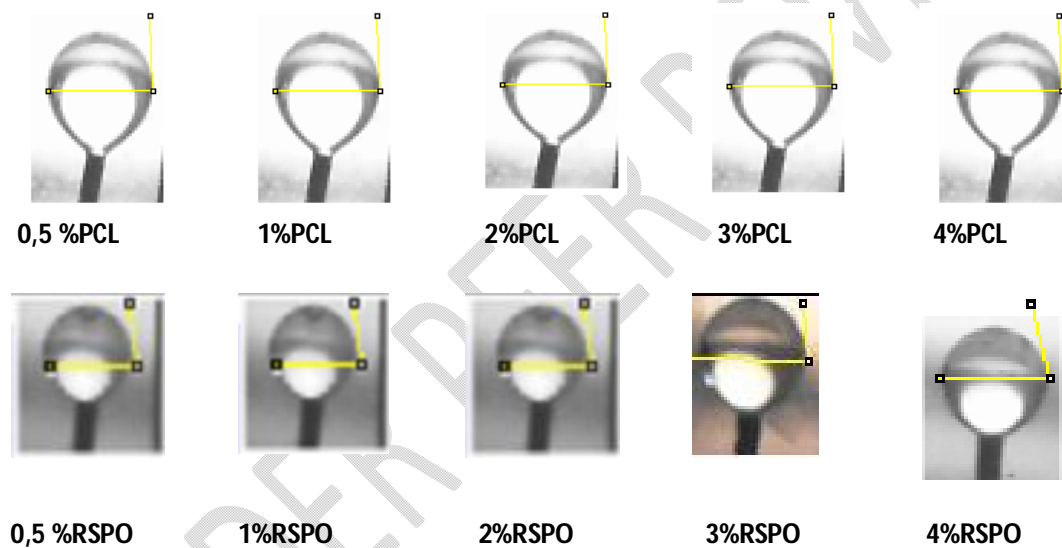
452 stabilized by bioderived particles. *RSC Advances* 11, 39027–39044.

453 <https://doi.org/10.1039/D1RA08086E>

454

455

456 ***Annexes***



457